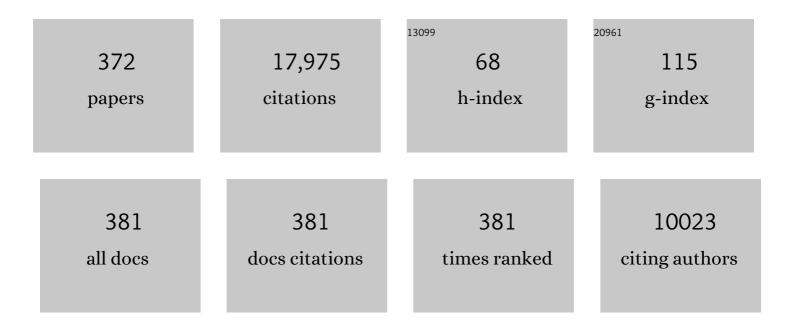
## Piotr J Slomka

List of Publications by Year in descending order

Source: https://exaly.com/author-pdf/5320355/publications.pdf Version: 2024-02-01



PIOTE SIOMEN

#	Article	IF	CITATIONS
1	Aortic 18F-sodium fluoride imaging. Journal of Nuclear Cardiology, 2023, 30, 811-813.	2.1	Ο
2	External validation of the CRAX2MACE model. Journal of Nuclear Cardiology, 2023, 30, 702-707.	2.1	5
3	Development and validation of ischemia risk scores. Journal of Nuclear Cardiology, 2023, 30, 324-334.	2.1	3
4	Automated nonlinear registration of coronary PET to CT angiography using pseudo-CT generated from PET with generative adversarial networks. Journal of Nuclear Cardiology, 2023, 30, 604-615.	2.1	11
5	Automated quantitative analysis of CZT SPECT stratifies cardiovascular risk in the obese population: Analysis of the REFINE SPECT registry. Journal of Nuclear Cardiology, 2022, 29, 727-736.	2.1	11
6	Quantitative Assessment of Cardiac Hypermetabolism and Perfusion for Diagnosis of Cardiac Sarcoidosis. Journal of Nuclear Cardiology, 2022, 29, 86-96.	2.1	20
7	Observer repeatability and interscan reproducibility of 18F-sodium fluoride coronary microcalcification activity. Journal of Nuclear Cardiology, 2022, 29, 126-135.	2.1	26
8	Respiration-averaged CT versus standard CT attenuation map for correction of 18F-sodium fluoride uptake in coronary atherosclerotic lesions on hybrid PET/CT. Journal of Nuclear Cardiology, 2022, 29, 430-439.	2.1	17
9	Quantifying microcalcification activity in the thoracic aorta. Journal of Nuclear Cardiology, 2022, 29, 1372-1385.	2.1	21
10	Prediction of 2-year major adverse cardiac events from myocardial perfusion scintigraphy and clinical risk factors. Journal of Nuclear Cardiology, 2022, 29, 1956-1963.	2.1	6
11	Machine Learning with <sup>18</sup> F-Sodium Fluoride PET and Quantitative Plaque Analysis on CT Angiography for the Future Risk of Myocardial Infarction. Journal of Nuclear Medicine, 2022, 63, 158-165.	5.0	34
12	Value of semiquantitative assessment of high-risk plaque features on coronary CT angiography over stenosis in selection of studies for FFRct. Journal of Cardiovascular Computed Tomography, 2022, 16, 27-33.	1.3	8
13	Diagnostic safety of a machine learning-based automatic patient selection algorithm for stress-only myocardial perfusion SPECT. Journal of Nuclear Cardiology, 2022, 29, 2295-2307.	2.1	21
14	Clinical Deployment of Explainable Artificial Intelligence of SPECT for Diagnosis of Coronary Artery Disease. JACC: Cardiovascular Imaging, 2022, 15, 1091-1102.	5.3	44
15	Determining a minimum set of variables for machine learning cardiovascular event prediction: results from REFINE SPECT registry. Cardiovascular Research, 2022, 118, 2152-2164.	3.8	26
16	Artificial intelligence-based attenuation correction; closer to clinical reality?. Journal of Nuclear Cardiology, 2022, 29, 2251-2253.	2.1	7
17	Improving detection accuracy of perfusion defect in standard dose SPECT-myocardial perfusion imaging by deep-learning denoising. Journal of Nuclear Cardiology, 2022, 29, 2340-2349.	2.1	5
18	Association of Myocardial Blood Flow Reserve With Adverse Left Ventricular Remodeling in Patients With Aortic Stenosis. JAMA Cardiology, 2022, 7, 93.	6.1	16

#	Article	IF	CITATIONS
19	Association of coronary artery calcium score with qualitatively and quantitatively assessed adverse plaque on coronary CT angiography in the SCOT-HEART trial. European Heart Journal Cardiovascular Imaging, 2022, 23, 1210-1221.	1.2	21
20	Prognostic value of early left ventricular ejection fraction reserve during regadenoson stress solid-state SPECT-MPI. Journal of Nuclear Cardiology, 2022, 29, 1219-1230.	2.1	5
21	Quantitative technetium pyrophosphate and cardiovascular magnetic resonance in patients with suspected cardiac amyloidosis. Journal of Nuclear Cardiology, 2022, 29, 2679-2690.	2.1	8
22	Detection of small coronary calcifications in patients with Agatston coronary artery calcium score of zero. Journal of Cardiovascular Computed Tomography, 2022, 16, 150-154.	1.3	7
23	The prevalence and predictors of inducible myocardial ischemia among patients referred for radionuclide stress testing. Journal of Nuclear Cardiology, 2022, 29, 2839-2849.	2.1	7
24	The Evolving Role of Artificial Intelligence in Cardiac Image Analysis. Canadian Journal of Cardiology, 2022, 38, 214-224.	1.7	8
25	Novel Techniques: Solid-State Detectors, Dose Reduction (SPECT/CT). , 2022, , 103-129.		0
26	Nuclear Medicine and Artificial Intelligence: Best Practices for Algorithm Development. Journal of Nuclear Medicine, 2022, 63, 500-510.	5.0	43
27	Artificial Intelligence and Cardiac PET/Computed Tomography Imaging. PET Clinics, 2022, 17, 85-94.	3.0	2
28	Comparison of diabetes to other prognostic predictors among patients referred for cardiac stress testing: A contemporary analysis from the REFINE SPECT Registry. Journal of Nuclear Cardiology, 2022, 29, 3003-3014.	2.1	6
29	18F-GP1 Positron Emission Tomography and Bioprosthetic Aortic Valve Thrombus. JACC: Cardiovascular Imaging, 2022, 15, 1107-1120.	5.3	12
30	Radiomics-Based Precision PhenotypingÂldentifies Unstable Coronary Plaques From Computed Tomography Angiography. JACC: Cardiovascular Imaging, 2022, 15, 859-871.	5.3	24
31	Aortic valve imaging using 18F-sodium fluoride: impact of triple motion correction. EJNMMI Physics, 2022, 9, 4.	2.7	3
32	The application of artificial intelligence in nuclear cardiology. Annals of Nuclear Medicine, 2022, 36, 111-122.	2.2	9
33	Intramyocardial Hemorrhage and the "Wave Front―of Reperfusion Injury Compromising Myocardial Salvage. Journal of the American College of Cardiology, 2022, 79, 35-48.	2.8	38
34	Association of Plaque Location and Vessel Geometry Determined by Coronary Computed Tomographic Angiography With Future Acute Coronary Syndrome–Causing Culprit Lesions. JAMA Cardiology, 2022, 7, 309.	6.1	13
35	Bypass Grafting and Native Coronary Artery Disease Activity. JACC: Cardiovascular Imaging, 2022, 15, 875-887.	5.3	24
36	Prevalence and predictors of automatically quantified myocardial ischemia within a multicenter international registry. Journal of Nuclear Cardiology, 2022, 29, 3221-3232.	2.1	3

#	Article	IF	CITATIONS
37	Thoracic Aortic 18F-Sodium Fluoride Activity and Ischemic Stroke in Patients With Established Cardiovascular Disease. JACC: Cardiovascular Imaging, 2022, 15, 1274-1288.	5.3	27
38	Future of nuclear cardiology is bright: Promise of cardiac PET/CT and artificial intelligence. Journal of Nuclear Cardiology, 2022, 29, 389-391.	2.1	3
39	Deep learning-enabled coronary CT angiography for plaque and stenosis quantification and cardiac risk prediction: an international multicentre study. The Lancet Digital Health, 2022, 4, e256-e265.	12.3	85
40	Calcium scoring in low-dose ungated chest CT scans using convolutional long-short term memory networks. , 2022, , .		2
41	Handling missing values in machine learning to predict patient-specific risk of adverse cardiac events: Insights from REFINE SPECT registry. Computers in Biology and Medicine, 2022, 145, 105449.	7.0	14
42	Improved myocardial blood flow estimation with residual activity correction and motion correction in 18F-flurpiridaz PET myocardial perfusion imaging. European Journal of Nuclear Medicine and Molecular Imaging, 2022, 49, 1881-1893.	6.4	9
43	Latest Advances in Multimodality Imaging of Aortic Stenosis. Journal of Nuclear Medicine, 2022, 63, 353-358.	5.0	14
44	Relationship between ischaemia, coronary artery calcium scores, and major adverse cardiovascular events. European Heart Journal Cardiovascular Imaging, 2022, 23, 1423-1433.	1.2	16
45	Pericoronary Adipose Tissue Attenuation, Low-Attenuation Plaque Burden, and 5-Year Risk of Myocardial Infarction. JACC: Cardiovascular Imaging, 2022, 15, 1078-1088.	5.3	46
46	Radiomorphological signs and clinical severity of SARS-CoV-2 lineage B.1.1.7. BJR   Open, 2022, 4, .	0.6	1
47	Artificial intelligence for disease diagnosis and risk prediction in nuclear cardiology. Journal of Nuclear Cardiology, 2022, 29, 1754-1762.	2.1	9
48	Explainable Deep Learning Improves Physician Interpretation of Myocardial Perfusion Imaging. Journal of Nuclear Medicine, 2022, , jnumed.121.263686.	5.0	7
49	Hepatosteatosis and Atherosclerotic Plaque at Coronary CT Angiography. Radiology: Cardiothoracic Imaging, 2022, 4, e210260.	2.5	6
50	Theme papers. Journal of Nuclear Cardiology, 2022, 29, 1753.	2.1	0
51	Quantifying sodium [18F]fluoride uptake in abdominal aortic aneurysms. EJNMMI Research, 2022, 12, .	2.5	2
52	<sup>18</sup> F-NaF PET/MRI for Detection of Carotid Atheroma in Acute Neurovascular Syndrome. Radiology, 2022, 305, 137-148.	7.3	7
53	Reproducibility of quantitative coronary calcium scoring from PET/CT attenuation maps: comparison to ECG-gated CT scans. European Journal of Nuclear Medicine and Molecular Imaging, 2022, 49, 4122-4132.	6.4	11
54	Plaque Burden and 1-Year Outcomes inÂAcute Chest Pain. JACC: Cardiovascular Imaging, 2022, 15, 1916-1925.	5.3	16

#	Article	IF	CITATIONS
55	Differences in Prognostic Value of Myocardial Perfusion Single-Photon Emission Computed Tomography Using High-Efficiency Solid-State Detector Between Men and Women in a Large International Multicenter Study. Circulation: Cardiovascular Imaging, 2022, 15, .	2.6	2
56	Machine learning to predict abnormal myocardial perfusion from pre-test features. Journal of Nuclear Cardiology, 2022, 29, 2393-2403.	2.1	7
57	Benefit of Early Revascularization Based on Inducible Ischemia and Left Ventricular Ejection Fraction. Journal of the American College of Cardiology, 2022, 80, 202-215.	2.8	19
58	Do we need dedicated cardiac SPECT systems?. Journal of Nuclear Cardiology, 2021, 28, 1331-1333.	2.1	2
59	Quantification of myocardial blood flow by CZT-SPECT with motion correction and comparison with 15O-water PET. Journal of Nuclear Cardiology, 2021, 28, 1477-1486.	2.1	31
60	Short-term repeatability of myocardial blood flow using 82Rb PET/CT: The effect of arterial input function position and motion correction. Journal of Nuclear Cardiology, 2021, 28, 1718-1725.	2.1	20
61	Myocardial blood flow: Is motion correction necessary?. Journal of Nuclear Cardiology, 2021, 28, 1347-1348.	2.1	0
62	Cardiovascular 18F-fluoride positron emission tomography-magnetic resonance imaging: A comparison study. Journal of Nuclear Cardiology, 2021, 28, 1-12.	2.1	25
63	Survival benefit of coronary revascularization after myocardial perfusion SPECT: The role of ischemia. Journal of Nuclear Cardiology, 2021, 28, 1676-1687.	2.1	11
64	CZT camera systems may provide better risk stratification for low-risk patients. Journal of Nuclear Cardiology, 2021, 28, 2927-2936.	2.1	9
65	Elucidating the pathophysiology of left bundle branch block related perfusion defects. Journal of Nuclear Cardiology, 2021, 28, 2923-2926.	2.1	1
66	Cardiac PET/MR: Are sophisticated attenuation correction techniques necessary for clinical routine assessments?. Journal of Nuclear Cardiology, 2021, 28, 2205-2206.	2.1	0
67	Repeatability of quantitative pericoronary adipose tissue attenuation and coronary plaque burden from coronary CT angiography. Journal of Cardiovascular Computed Tomography, 2021, 15, 81-84.	1.3	35
68	Is SPECT LVEF assessment more accurate than CT at higher heart rates? More evidence for complementary information in multimodality imaging. Journal of Nuclear Cardiology, 2021, 28, 317-319.	2.1	0
69	Prognostically safe stress-only single-photon emission computed tomography myocardial perfusion imaging guided by machine learning: report from REFINE SPECT. European Heart Journal Cardiovascular Imaging, 2021, 22, 705-714.	1.2	38
70	Machine Learning Adds to Clinical and CAC Assessments in Predicting 10-Year CHD and CVD Deaths. JACC: Cardiovascular Imaging, 2021, 14, 615-625.	5.3	52
71	Quantitative clinical nuclear cardiology, part 2: Evolving/emerging applications. Journal of Nuclear Cardiology, 2021, 28, 115-127.	2.1	15
72	Quantitative clinical nuclear cardiology, part 2: Evolving/emerging applications. Journal of Nuclear Medicine, 2021, 62, 168-176.	5.0	5

#	Article	IF	CITATIONS
73	Machine learning integration of circulating and imaging biomarkers for explainable patient-specific prediction of cardiac events: A prospective study. Atherosclerosis, 2021, 318, 76-82.	0.8	37
74	Non-calcific aortic tissue quantified from computed tomography angiography improves diagnosis and prognostication of patients referred for transcatheter aortic valve implantation. European Heart Journal Cardiovascular Imaging, 2021, 22, 626-635.	1.2	16
75	Epicardial adipose tissue is associated with extent of pneumonia and adverse outcomes in patients with COVID-19. Metabolism: Clinical and Experimental, 2021, 115, 154436.	3.4	48
76	Preprint manuscripts and servers in the era of coronavirus disease 2019. Journal of Evaluation in Clinical Practice, 2021, 27, 16-21.	1.8	26
77	Prediction of revascularization by coronary CT angiography using a machine learning ischemia risk score. European Radiology, 2021, 31, 1227-1235.	4.5	15
78	Beware the pitfalls of beauty: High-quality myocardial images with resolution recovery. Journal of Nuclear Cardiology, 2021, 28, 245-248.	2.1	4
79	Advances in Quantitative Analysis of <sup>18</sup> F-Sodium Fluoride Coronary Imaging. Molecular Imaging, 2021, 2021, 8849429.	1.4	8
80	Artificial Intelligence in Cardiovascular Imaging for Risk Stratification in Coronary Artery Disease. Radiology: Cardiothoracic Imaging, 2021, 3, e200512.	2.5	39
81	Practical Guide for Interpreting and Reporting Cardiac PET Measurements of Myocardial Blood Flow: An Information Statement from the American Society of Nuclear Cardiology, and the Society of Nuclear Medicine and Molecular Imaging. Journal of Nuclear Medicine, 2021, 62, 1599-1615.	5.0	13
82	Quantitation of Poststress Change in Ventricular Morphology Improves Risk Stratification. Journal of Nuclear Medicine, 2021, 62, 1582-1590.	5.0	7
83	Practical guide for interpreting and reporting cardiac PET measurements of myocardial blood flow: an Information Statement from the American Society of Nuclear Cardiology, and the Society of Nuclear Medicine and Molecular Imaging. Journal of Nuclear Cardiology, 2021, 28, 768-787.	2.1	28
84	Artificial intelligence in cardiovascular CT: Current status and future implications. Journal of Cardiovascular Computed Tomography, 2021, 15, 462-469.	1.3	20
85	Diagnostic and prognostic value of Technetium-99m pyrophosphate uptake quantitation for transthyretin cardiac amyloidosis. Journal of Nuclear Cardiology, 2021, 28, 1835-1845.	2.1	27
86	Impact of Early Revascularization on Major Adverse Cardiovascular Events inÂRelation to Automatically QuantifiedÂlschemia. JACC: Cardiovascular Imaging, 2021, 14, 644-653.	5.3	28
87	Position paper of the EACVI and EANM on artificial intelligence applications in multimodality cardiovascular imaging using SPECT/CT, PET/CT, and cardiac CT. European Journal of Nuclear Medicine and Molecular Imaging, 2021, 48, 1399-1413.	6.4	45
88	Clinical Utility of SPECT in the Heart Transplant Population. Transplantation, 2021, Publish Ahead of Print, .	1.0	4
89	155â€Pericoronary adipose tissue attenuation, low attenuation plaque burden and 5-year risk of myocardial infarction. , 2021, , .		0
90	157â€18F-sodium fluoride positron emission tomography, aortic disease activity and ischaemic stroke		0

risk. , 2021, , .

#	Article	IF	CITATIONS
91	Impact of train/test sample regimen on performance estimate stability of machine learning in cardiovascular imaging. Scientific Reports, 2021, 11, 14490.	3.3	23
92	Reproducibility of quantitative plaque measurement in advanced coronary artery disease. Journal of Cardiovascular Computed Tomography, 2021, 15, 333-338.	1.3	24
93	Prognostic Value of Phase Analysis for Predicting Adverse Cardiac Events Beyond Conventional Single-Photon Emission Computed Tomography Variables: Results From the REFINE SPECT Registry. Circulation: Cardiovascular Imaging, 2021, 14, e012386.	2.6	13
94	Pericoronary and periaortic adipose tissue density are associated with inflammatory disease activity in Takayasu arteritis and atherosclerosis. European Heart Journal Open, 2021, 1, oeab019.	2.3	15
95	Native Aortic Valve Disease Progression and Bioprosthetic Valve Degeneration in Patients With Transcatheter Aortic Valve Implantation. Circulation, 2021, 144, 1396-1408.	1.6	32
96	Sex-Specific Computed Tomography Coronary Plaque Characterization and Risk of Myocardial Infarction. JACC: Cardiovascular Imaging, 2021, 14, 1804-1814.	5.3	28
97	Assessing Performance of Machine Learning. JAMA Cardiology, 2021, 6, 1465.	6.1	3
98	Metabolic syndrome, fatty liver, and artificial intelligence-based epicardial adipose tissue measures predict long-term risk of cardiac events: a prospective study. Cardiovascular Diabetology, 2021, 20, 27.	6.8	33
99	Contrast-enhanced computed tomography assessment of aortic stenosis. Heart, 2021, 107, 1905-1911.	2.9	32
100	Simulation of Low-Dose Protocols for Myocardial Perfusion <sup>82</sup> Rb Imaging. Journal of Nuclear Medicine, 2021, 62, 1112-1117.	5.0	6
101	Noncalcified plaque burden quantified from coronary computed tomography angiography improves prediction of side branch occlusion after main vessel stenting in bifurcation lesions: results from the CT-PRECISION registry. Clinical Research in Cardiology, 2021, 110, 114-123.	3.3	5
102	Evaluation of the effect of reducing administered activity on assessment of function in cardiac gated SPECT. Journal of Nuclear Cardiology, 2020, 27, 562-572.	2.1	6
103	Analytical quantification of aortic valve 18F-sodium fluoride PET uptake. Journal of Nuclear Cardiology, 2020, 27, 962-972.	2.1	32
104	CRAX: A simple cardiovascular risk assessment tool to predict risk of acute myocardial infarction or death. Journal of Nuclear Cardiology, 2020, 27, 2365-2374.	2.1	8
105	Upper reference limits of transient ischemic dilation ratio for different protocols on new-generation cadmium zinc telluride cameras: A report from REFINE SPECT registry. Journal of Nuclear Cardiology, 2020, 27, 1180-1189.	2.1	17
106	Predictors of 18F-sodium fluoride uptake in patients with stable coronary artery disease and adverse plaque features on computed tomography angiography. European Heart Journal Cardiovascular Imaging, 2020, 21, 58-66.	1.2	50
107	Simultaneous Tc-99m PYP/Tl-201 dual-isotope SPECT myocardial imaging in patients with suspected cardiac amyloidosis. Journal of Nuclear Cardiology, 2020, 27, 28-37.	2.1	25
108	Software reproducibility of myocardial blood flow and flow reserve quantification in ischemic heart disease: A 13N-ammonia PET study. Journal of Nuclear Cardiology, 2020, 27, 1225-1233.	2.1	14

#	Article	IF	CITATIONS
109	Optimization of reconstruction and quantification of motion-corrected coronary PET-CT. Journal of Nuclear Cardiology, 2020, 27, 494-504.	2.1	43
110	Rationale and design of the REgistry of Fast Myocardial Perfusion Imaging with NExt generation SPECT (REFINE SPECT). Journal of Nuclear Cardiology, 2020, 27, 1010-1021.	2.1	74
111	Reply: Clarifying the Utility of Myocardial Blood Flow and Myocardial Flow Reserve After Cardiac Transplantation. Journal of Nuclear Medicine, 2020, 61, 620.2-622.	5.0	0
112	5-Year Prognostic Value of QuantitativeÂVersus Visual MPI in SubtleÂPerfusionÂDefects. JACC: Cardiovascular Imaging, 2020, 13, 774-785.	5.3	70
113	Machine learning predicts per-vessel early coronary revascularization after fast myocardial perfusion SPECT: results from multicentre REFINE SPECT registry. European Heart Journal Cardiovascular Imaging, 2020, 21, 549-559.	1.2	70
114	Comparative Prognostic and Diagnostic Value of Myocardial Blood Flow and Myocardial Flow Reserve After Cardiac Transplantation. Journal of Nuclear Medicine, 2020, 61, 249-255.	5.0	28
115	Quantitative Clinical Nuclear Cardiology, Part 1: Established Applications. Journal of Nuclear Cardiology, 2020, 27, 189-201.	2.1	15
116	Whole-vessel coronary 18F-sodium fluoride PET for assessment of the global coronary microcalcification burden. European Journal of Nuclear Medicine and Molecular Imaging, 2020, 47, 1736-1745.	6.4	50
117	Machine learning to predict the long-term risk of myocardial infarction and cardiac death based on clinical risk, coronary calcium, and epicardial adipose tissue: a prospective study. Cardiovascular Research, 2020, 116, 2216-2225.	3.8	78
118	Vulnerable plaque imaging using <sup>18</sup> F-sodium fluoride positron emission tomography. British Journal of Radiology, 2020, 93, 20190797.	2.2	22
119	Coronary computed tomography–angiography quantitative plaque analysis improves detection of early cardiac allograft vasculopathy: A pilot study. American Journal of Transplantation, 2020, 20, 1375-1383.	4.7	13
120	Myocardial Ischemic Burden and Differences in Prognosis Among Patients With and Without Diabetes: Results From the Multicenter International REFINE SPECT Registry. Diabetes Care, 2020, 43, 453-459.	8.6	21
121	Quantitative Burden of COVID-19 Pneumonia at Chest CT Predicts Adverse Outcomes: A Post Hoc Analysis of a Prospective International Registry. Radiology: Cardiothoracic Imaging, 2020, 2, e200389.	2.5	32
122	Proposed Requirements for Cardiovascular Imaging-Related Machine Learning Evaluation (PRIME): A Checklist. JACC: Cardiovascular Imaging, 2020, 13, 2017-2035.	5.3	123
123	Response to the letter to the editor: Lassen et al. 3D PET/CT 82Rb PET myocardial blood flow quantification: comparison of half-dose and full-dose protocols. European Journal of Nuclear Medicine and Molecular Imaging, 2020, 47, 2731-2732.	6.4	0
124	Coronary <sup>18</sup> F-Fluoride Uptake and Progression of Coronary Artery Calcification. Circulation: Cardiovascular Imaging, 2020, 13, e011438.	2.6	43
125	Coronary 18F-Sodium Fluoride Uptake Predicts Outcomes in Patients With Coronary Artery Disease. Journal of the American College of Cardiology, 2020, 75, 3061-3074.	2.8	100
126	Artificial intelligence: improving the efficiency of cardiovascular imaging. Expert Review of Medical Devices, 2020, 17, 565-577.	2.8	20

#	Article	IF	CITATIONS
127	18F-SODIUM FLUORIDE CORONARY UPTAKE PREDICTS MYOCARDIAL INFARCTIONS IN PATIENTS WITH KNOWN CORONARY ARTERY DISEASE. Journal of the American College of Cardiology, 2020, 75, 3667.	2.8	5
128	PET-derived bone information from 18F-sodium fluoride: A perfect match for whole-body PET/MR attenuation correction?. Journal of Nuclear Cardiology, 2020, 27, 1142-1144.	2.1	0
129	Low-Attenuation Noncalcified Plaque on Coronary Computed Tomography Angiography Predicts Myocardial Infarction. Circulation, 2020, 141, 1452-1462.	1.6	348
130	Heart Rateâ^'Independent 3D Myocardial Blood Oxygen Levelâ^'Dependent MRI at 3.0 T with Simultaneous <sup>13</sup> Nâ^'Ammonia PET Validation. Radiology, 2020, 295, 82-93.	7.3	10
131	3D PET/CT 82Rb PET myocardial blood flow quantification: comparison of half-dose and full-dose protocols. European Journal of Nuclear Medicine and Molecular Imaging, 2020, 47, 3084-3093.	6.4	10
132	Taking pigeons to heart: Birds proficiently diagnose human cardiac disease. Learning and Behavior, 2020, 48, 9-21.	1.0	4
133	Deep Learning–Based Quantification of Epicardial Adipose Tissue Volume and Attenuation Predicts Major Adverse Cardiovascular Events in Asymptomatic Subjects. Circulation: Cardiovascular Imaging, 2020, 13, e009829.	2.6	77
134	Prognostic significance of previous myocardial infarction and previous revascularization in patients undergoing SPECT MPI. International Journal of Cardiology, 2020, 313, 9-15.	1.7	19
135	Transient ischaemic dilation and post-stress wall motion abnormality increase risk in patients with less than moderate ischaemia: analysis of the REFINE SPECT registry. European Heart Journal Cardiovascular Imaging, 2020, 21, 567-575.	1.2	21
136	Myocardial Infarction Associates With a Distinct Pericoronary Adipose Tissue Radiomic Phenotype. JACC: Cardiovascular Imaging, 2020, 13, 2371-2383.	5.3	86
137	Application and Translation of Artificial Intelligence to Cardiovascular Imaging in Nuclear Medicine and Noncontrast CT. Seminars in Nuclear Medicine, 2020, 50, 357-366.	4.6	23
138	Clinical applications of machine learning in cardiovascular disease and its relevance to cardiac imaging. European Heart Journal, 2019, 40, 1975-1986.	2.2	327
139	Improving perfusion defect detection with respiratory motion correction in cardiac SPECT at standard and reduced doses. Journal of Nuclear Cardiology, 2019, 26, 1526-1538.	2.1	4
140	Triple-gated motion and blood pool clearance corrections improve reproducibility of coronary 18F-NaF PET. European Journal of Nuclear Medicine and Molecular Imaging, 2019, 46, 2610-2620.	6.4	45
141	Solid-State Detector SPECT Myocardial Perfusion Imaging. Journal of Nuclear Medicine, 2019, 60, 1194-1204.	5.0	57
142	Quantitative Clinical Nuclear Cardiology, Part 1: Established Applications. Journal of Nuclear Medicine, 2019, 60, 1507-1516.	5.0	16
143	Selection of abstracts from the scientific sessions of The Society Of Nuclear Medicine and Molecular Imaging annual meeting Anaheim CA. Journal of Nuclear Cardiology, 2019, 26, 1667-1673.	2.1	0
144	Leveraging latest computer science tools to advance nuclear cardiology. Journal of Nuclear Cardiology, 2019, 26, 1501-1504.	2.1	2

#	Article	IF	CITATIONS
145	Accurate needle-free assessment of myocardial oxygenation for ischemic heart disease in canines using magnetic resonance imaging. Science Translational Medicine, 2019, 11, .	12.4	12
146	Myocardial Blood Flow Quantification With Dynamic Contrast-Enhanced Computed Tomography. Circulation: Cardiovascular Imaging, 2019, 12, e009431.	2.6	1
147	Standardized volumetric plaque quantification and characterization from coronary CT angiography: a head-to-head comparison with invasive intravascular ultrasound. European Radiology, 2019, 29, 6129-6139.	4.5	50
148	Gating Approaches in Cardiac PET Imaging. PET Clinics, 2019, 14, 271-279.	3.0	19
149	Artificial Intelligence in Cardiovascular Imaging. Journal of the American College of Cardiology, 2019, 73, 1317-1335.	2.8	374
150	Decrease in LDL-C is associated with decrease in all components of noncalcified plaque on coronary CTA. Atherosclerosis, 2019, 285, 128-134.	0.8	6
151	Effect of tube potential and luminal contrast attenuation on atherosclerotic plaque attenuation by coronary CT angiography: In vivo comparison with intravascular ultrasound. Journal of Cardiovascular Computed Tomography, 2019, 13, 219-225.	1.3	14
152	Relationship between changes in pericoronary adipose tissue attenuation and coronary plaque burden quantified from coronary computed tomography angiography. European Heart Journal Cardiovascular Imaging, 2019, 20, 636-643.	1.2	129
153	Peri-Coronary Adipose Tissue Density IsÂAssociated With 18F-Sodium Fluoride Coronary Uptake in Stable Patients WithÂHigh-Risk Plaques. JACC: Cardiovascular Imaging, 2019, 12, 2000-2010.	5.3	129
154	Improved Evaluation of Lipid-Rich Plaque at Coronary CT Angiography: Head-to-Head Comparison with Intravascular US. Radiology: Cardiothoracic Imaging, 2019, 1, e190069.	2.5	9
155	Fully Automated CT Quantification of Epicardial Adipose Tissue by Deep Learning: A Multicenter Study. Radiology: Artificial Intelligence, 2019, 1, e190045.	5.8	83
156	Three-Hour Delayed Imaging Improves Assessment of Coronary <sup>18</sup> F-Sodium Fluoride PET. Journal of Nuclear Medicine, 2019, 60, 530-535.	5.0	44
157	Data-Driven Gross Patient Motion Detection and Compensation: Implications for Coronary <sup>18</sup> F-NaF PET Imaging. Journal of Nuclear Medicine, 2019, 60, 830-836.	5.0	39
158	Cardiac motion correction for improving perfusion defect detection in cardiac SPECT at standard and reduced doses of activity. Physics in Medicine and Biology, 2019, 64, 055005.	3.0	7
159	Deep Learning Analysis of Upright-Supine High-Efficiency SPECT Myocardial Perfusion Imaging for Prediction of Obstructive Coronary Artery Disease: A Multicenter Study. Journal of Nuclear Medicine, 2019, 60, 664-670.	5.0	113
160	Making the invisible visible: Phase dyssynchrony has potential as a new prognostic marker. Journal of Nuclear Cardiology, 2019, 26, 298-302.	2.1	9
161	Assessing LV remodeling in nuclear cardiology. Journal of Nuclear Cardiology, 2019, 26, 233-235.	2.1	3
162	Prediction of cardiac death after adenosine myocardial perfusion SPECT based on machine learning. Journal of Nuclear Cardiology, 2019, 26, 1746-1754.	2.1	57

#	Article	IF	CITATIONS
163	Deep learning-based stenosis quantification from coronary CT angiography. , 2019, 10949, .		27
164	Reasons and implications of agreements and disagreements between coronary flow reserve, fractional flow reserve, and myocardial perfusion imaging. Journal of Nuclear Cardiology, 2018, 25, 104-119.	2.1	16
165	Combined evaluation of regional coronary artery calcium and myocardial perfusion by 82Rb PET/CT in the identification of obstructive coronary artery disease. European Journal of Nuclear Medicine and Molecular Imaging, 2018, 45, 521-529.	6.4	58
166	Deep Learning for Quantification of Epicardial and Thoracic Adipose Tissue From Non-Contrast CT. IEEE Transactions on Medical Imaging, 2018, 37, 1835-1846.	8.9	135
167	New Trends in Quantitative Nuclear Cardiology Methods. Current Cardiovascular Imaging Reports, 2018, 11, 1.	0.6	16
168	Integrated prediction of lesion-specific ischaemia from quantitative coronary CT angiography using machine learning: a multicentre study. European Radiology, 2018, 28, 2655-2664.	4.5	135
169	Clinical Quantification of Myocardial Blood Flow Using PET: Joint Position Paper of the SNMMI Cardiovascular Council and the ASNC. Journal of Nuclear Cardiology, 2018, 25, 269-297.	2.1	151
170	Deep Learning for Prediction of Obstructive Disease From Fast Myocardial Perfusion SPECT. JACC: Cardiovascular Imaging, 2018, 11, 1654-1663.	5.3	246
171	Factors affecting appearance of a normal myocardial perfusion scan. Journal of Nuclear Cardiology, 2018, 25, 1655-1657.	2.1	Ο
172	Fully automated analysis of attenuation-corrected SPECT for the long-term prediction of acute myocardial infarction. Journal of Nuclear Cardiology, 2018, 25, 1353-1360.	2.1	17
173	Automatic determination of cardiovascular risk by CT attenuation correction maps in Rb-82 PET/CT. Journal of Nuclear Cardiology, 2018, 25, 2133-2142.	2.1	49
174	Hybrid quantitative imaging: Will it enter clinical practice?. Journal of Nuclear Cardiology, 2018, 25, 1387-1389.	2.1	2
175	Investigation of dose reduction in cardiac perfusion SPECT via optimization and choice of the image reconstruction strategy. Journal of Nuclear Cardiology, 2018, 25, 2117-2128.	2.1	35
176	Prognostic Value of Combined Clinical andÂMyocardial Perfusion Imaging Data Using Machine Learning. JACC: Cardiovascular Imaging, 2018, 11, 1000-1009.	5.3	172
177	Epicardial adipose tissue density and volume are related to subclinical atherosclerosis, inflammation and major adverse cardiac events in asymptomatic subjects. Journal of Cardiovascular Computed Tomography, 2018, 12, 67-73.	1.3	143
178	Clinical Quantification of Myocardial Blood Flow Using PET: Joint Position Paper of the SNMMI Cardiovascular Council and the ASNC. Journal of Nuclear Medicine, 2018, 59, 273-293.	5.0	163
179	Impact of incomplete ventricular coverage on diagnostic performance of myocardial perfusion imaging. International Journal of Cardiovascular Imaging, 2018, 34, 661-669.	1.5	6
180	Dual-isotope myocardial perfusion SPECT imaging: Past, present, and future. Journal of Nuclear Cardiology, 2018, 25, 2024-2028.	2.1	5

#	Article	IF	CITATIONS
181	Feasibility of Coronary <sup>18</sup> F-Sodium Fluoride Positron-Emission Tomography Assessment With the Utilization of Previously Acquired Computed Tomography Angiography. Circulation: Cardiovascular Imaging, 2018, 11, e008325.	2.6	36
182	Single Photon Emission Computed Tomography (SPECT) Myocardial Perfusion Imaging Guidelines: Instrumentation, Acquisition, Processing, and Interpretation. Journal of Nuclear Cardiology, 2018, 25, 1784-1846.	2.1	241
183	Non-invasive fractional flow reserve in vessels without severe obstructive stenosis is associated with coronary plaque burden. Journal of Cardiovascular Computed Tomography, 2018, 12, 379-384.	1.3	17
184	Pericoronary Adipose Tissue Computed Tomography Attenuation and High-Risk Plaque Characteristics in Acute Coronary Syndrome Compared With Stable Coronary Artery Disease. JAMA Cardiology, 2018, 3, 858.	6.1	186
185	Improvement in LDL is associated with decrease in non-calcified plaque volume on coronary CTA as measured by automated quantitative software. Journal of Cardiovascular Computed Tomography, 2018, 12, 385-390.	1.3	21
186	Machine learning for predicting death and heart attacks from CCTA. Journal of Cardiovascular Computed Tomography, 2018, 12, 210-211.	1.3	1
187	Machine learning for prediction of all-cause mortality in patients with suspected coronary artery disease: a 5-year multicentre prospective registry analysis. European Heart Journal, 2017, 38, ehw188.	2.2	447
188	Multicenter evaluation of stress-first myocardial perfusion image triage by nuclear technologists and automated quantification. Journal of Nuclear Cardiology, 2017, 24, 809-820.	2.1	5
189	Myocardial blood flow from SPECT. Journal of Nuclear Cardiology, 2017, 24, 278-281.	2.1	11
190	Optimizing radiation dose and imaging time with conventional myocardial perfusion SPECT: Technical aspects. Journal of Nuclear Cardiology, 2017, 24, 888-891.	2.1	16
191	Normal limits for transient ischemic dilation with 99mTc myocardial perfusion SPECT protocols. Journal of Nuclear Cardiology, 2017, 24, 1709-1711.	2.1	8
192	Quantification with normal limits: New cameras and low-dose imaging. Journal of Nuclear Cardiology, 2017, 24, 1637-1640.	2.1	8
193	Cardiac imaging: working towards fully-automated machine analysis & interpretation. Expert Review of Medical Devices, 2017, 14, 197-212.	2.8	78
194	Molecular Imaging of Vulnerable Coronary Plaque: A Pathophysiologic Perspective. Journal of Nuclear Medicine, 2017, 58, 359-364.	5.0	20
195	Enhancing Cardiac PET by Motion Correction Techniques. Current Cardiology Reports, 2017, 19, 14.	2.9	34
196	Motion-Corrected Imaging of the Aortic Valve with <sup>18</sup> F-NaF PET/CT and PET/MRI: A Feasibility Study. Journal of Nuclear Medicine, 2017, 58, 1811-1814.	5.0	23
197	Arterial CO <sub>2</sub> as a Potent Coronary Vasodilator: A Preclinical PET/MR Validation Study with Implications for Cardiac Stress Testing. Journal of Nuclear Medicine, 2017, 58, 953-960.	5.0	14
198	Quantitative plaque features from coronary computed tomography angiography to identify regional ischemia by myocardial perfusion imaging. European Heart Journal Cardiovascular Imaging, 2017, 18, 499-507.	1.2	31

#	Article	IF	CITATIONS
199	Technical consideration for dual ECG/respiratory-gated cardiac PET imaging. Journal of Nuclear Cardiology, 2017, 24, 1246-1252.	2.1	4
200	Comparison of the Coronary Artery Calcium Score and Number of Calcified Coronary Plaques for Predicting Patient Mortality Risk. American Journal of Cardiology, 2017, 120, 2154-2159.	1.6	27
201	Quantitative global plaque characteristics from coronary computed tomography angiography for the prediction of future cardiac mortality during long-term follow-up. European Heart Journal Cardiovascular Imaging, 2017, 18, 1331-1339.	1.2	90
202	Status of cardiovascular PET radiation exposure and strategies for reduction: An Information Statement from the Cardiovascular PET Task Force. Journal of Nuclear Cardiology, 2017, 24, 1427-1439.	2.1	24
203	Automatic Valve Plane Localization in Myocardial Perfusion SPECT/CT by Machine Learning: Anatomic and Clinical Validation. Journal of Nuclear Medicine, 2017, 58, 961-967.	5.0	56
204	How to reconstruct dynamic cardiac PET data?. Journal of Nuclear Cardiology, 2017, 24, 291-293.	2.1	1
205	Evaluation of a strategy to find personalized, patient-specific injected activity levels for SPECT-MPI. , 2017, , .		1
206	The Status and Future of PET Myocardial Blood Flow Quantification Software. Annals of Nuclear Cardiology, 2016, 2, 106-110.	0.2	10
207	Novel SPECT Technologies and Approaches in Cardiac Imaging. Cardiovascular Innovations and Applications, 2016, 2, 31-46.	0.3	9
208	Extending the Use of Coronary Calcium Scanning to Clinical Rather Than Just Screening Populations. Circulation: Cardiovascular Imaging, 2016, 9, .	2.6	7
209	Imaging of coronary atherosclerosis — evolution towards new treatment strategies. Nature Reviews Cardiology, 2016, 13, 533-548.	13.7	47
210	Epicardial adipose tissue volume but not density is an independent predictor for myocardial ischemia. Journal of Cardiovascular Computed Tomography, 2016, 10, 141-149.	1.3	49
211	Demons versus level-set motion registration for coronary <sup>18</sup> F-sodium fluoride PET. Proceedings of SPIE, 2016, 9784, .	0.8	11
212	Value Based Imaging for Coronary Artery Disease: Implications for Nuclear Cardiology and Cardiac CT. , 2016, , 349-380.		0
213	Normal Databases for the Relative Quantification of Myocardial Perfusion. Current Cardiovascular Imaging Reports, 2016, 9, 1.	0.6	18
214	Quantitation of left ventricular ejection fraction reserve from early gated regadenoson stress Tc-99m high-efficiency SPECT. Journal of Nuclear Cardiology, 2016, 23, 1251-1261.	2.1	25
215	"Same-Patient Processing―for multiple cardiac SPECT studies. 1. Improving LV segmentation accuracy. Journal of Nuclear Cardiology, 2016, 23, 1435-1441.	2.1	11
216	"Same-patient processing―for multiple cardiac SPECT studies. 2. Improving quantification repeatability. Journal of Nuclear Cardiology, 2016, 23, 1442-1453.	2.1	11

#	Article	IF	CITATIONS
217	Automatic detection of cardiovascular risk in CT attenuation correction maps in Rb-82 PET/CTs. Proceedings of SPIE, 2016, , .	0.8	2
218	Predictors of high-risk coronary artery disease in subjects with normal SPECT myocardial perfusion imaging. Journal of Nuclear Cardiology, 2016, 23, 530-541.	2.1	39
219	Automated pericardial fat quantification from coronary magnetic resonance angiography: feasibility study. Journal of Medical Imaging, 2016, 3, 014002.	1.5	7
220	Motion Correction of <sup>18</sup> F-NaF PET for Imaging Coronary Atherosclerotic Plaques. Journal of Nuclear Medicine, 2016, 57, 54-59.	5.0	74
221	Recent Advances and Future Progress in PET Instrumentation. Seminars in Nuclear Medicine, 2016, 46, 5-19.	4.6	147
222	Automated Quantitative Nuclear Cardiology Methods. Cardiology Clinics, 2016, 34, 47-57.	2.2	14
223	Frontiers of Nuclear Cardiology. Cardiology Clinics, 2016, 34, xiii.	2.2	1
224	Technical Aspects of Cardiac PET Imaging and Recent Advances. Cardiology Clinics, 2016, 34, 13-23.	2.2	5
225	Imaging moving heart structures with PET. Journal of Nuclear Cardiology, 2016, 23, 486-490.	2.1	5
226	Automated pericardium delineation and epicardial fat volume quantification from noncontrast CT. Medical Physics, 2015, 42, 5015-5026.	3.0	32
227	Coronary Artery Calcification, Epicardial Fat Burden, and Cardiovascular Events in Chronic Obstructive Pulmonary Disease. PLoS ONE, 2015, 10, e0126613.	2.5	23
228	Advances in SPECT and PET Hardware. Progress in Cardiovascular Diseases, 2015, 57, 566-578.	3.1	73
229	Dual-Gated Motion-Frozen Cardiac PET with Flurpiridaz F 18. Journal of Nuclear Medicine, 2015, 56, 1876-1881.	5.0	45
230	Prediction of revascularization after myocardial perfusion SPECT by machine learning in a large population. Journal of Nuclear Cardiology, 2015, 22, 877-884.	2.1	110
231	Quantitative high-efficiency cadmium-zinc-telluride SPECT with dedicated parallel-hole collimation system in obese patients: Results of a multi-center study. Journal of Nuclear Cardiology, 2015, 22, 266-275.	2.1	45
232	Structured learning algorithm for detection of nonobstructive and obstructive coronary plaque lesions from computed tomography angiography. Journal of Medical Imaging, 2015, 2, 014003.	1.5	71
233	Coronary calcium scoring from contrast coronary CT angiography using a semiautomated standardized method. Journal of Cardiovascular Computed Tomography, 2015, 9, 446-453.	1.3	25
234	Automated Quantitative Plaque Burden from Coronary CT Angiography Noninvasively Predicts Hemodynamic Significance by using Fractional Flow Reserve in Intermediate Coronary Lesions. Radiology, 2015, 276, 408-415.	7.3	67

#	Article	IF	CITATIONS
235	Automatic registration of misaligned CT attenuation correction maps in Rb-82 PET/CT improves detection of angiographically significant coronary artery disease. Journal of Nuclear Cardiology, 2015, 22, 1285-1295.	2.1	33
236	Relationship Between Quantitative Adverse Plaque Features From Coronary Computed Tomography Angiography and Downstream Impaired Myocardial Flow Reserve by <sup>13</sup> N-Ammonia Positron Emission Tomography. Circulation: Cardiovascular Imaging, 2015, 8, e003255.	2.6	55
237	Combined Quantitative Assessment of Myocardial Perfusion and Coronary Artery Calcium Score by Hybrid <sup>82</sup> Rb PET/CT Improves Detection of Coronary Artery Disease. Journal of Nuclear Medicine, 2015, 56, 1345-1350.	5.0	50
238	Relationship of epicardial fat volume from noncontrast CT with impaired myocardial flow reserve by positron emission tomography. Journal of Cardiovascular Computed Tomography, 2015, 9, 303-309.	1.3	23
239	Extensive thoracic aortic calcification is an independent predictor of development of coronary artery calcium among individuals with coronary artery calcium score of zero. Atherosclerosis, 2015, 238, 4-8.	0.8	15
240	Absolute myocardial blood flow quantification with SPECT/CT: Is it possible?. Journal of Nuclear Cardiology, 2014, 21, 1092-1095.	2.1	22
241	Quantification of I-123-meta-iodobenzylguanidine Heart-to-Mediastinum Ratios: Not So Simple After All. Journal of Nuclear Cardiology, 2014, 21, 979-983.	2.1	14
242	Clinical value of supine and upright myocardial perfusion imaging in obese patients using the D-SPECT camera. Journal of Nuclear Cardiology, 2014, 21, 478-485.	2.1	42
243	Motivation for whole-heart perfusion CMR: a simulation study based on retrospective comparison of the diagnostic performance of 3-slice vs. whole-heart SPECT. Journal of Cardiovascular Magnetic Resonance, 2014, 16, O99.	3.3	Ο
244	Quantification of Myocardial Blood Flow inÂAbsolute Terms Using 82Rb PET Imaging. JACC: Cardiovascular Imaging, 2014, 7, 1119-1127.	5.3	144
245	Interscan reproducibility of quantitative coronary plaque volume and composition from CT coronary angiography using an automated method. European Radiology, 2014, 24, 2300-2308.	4.5	49
246	Achieving Very-Low-Dose Radiation Exposure in Cardiac Computed Tomography, Single-Photon Emission Computed Tomography, and Positron Emission Tomography. Circulation: Cardiovascular Imaging, 2014, 7, 723-734.	2.6	15
247	The role of PET quantification in cardiovascular imaging. Clinical and Translational Imaging, 2014, 2, 343-358.	2.1	40
248	New Cardiac Cameras: Single-Photon Emission CT and PET. Seminars in Nuclear Medicine, 2014, 44, 232-251.	4.6	65
249	Comparison of Image Quality, Myocardial Perfusion, and Left Ventricular Function Between Standard Imaging and Single-Injection Ultra-Low-Dose Imaging Using a High-Efficiency SPECT Camera: The MILLISIEVERT Study. Journal of Nuclear Medicine, 2014, 55, 1430-1437.	5.0	87
250	Comparison of quantitative atherosclerotic plaque burden from coronary CT angiography in patients with first acute coronary syndrome and stable coronary artery disease. Journal of Cardiovascular Computed Tomography, 2014, 8, 368-374.	1.3	68
251	Two-position supine/prone myocardial perfusion SPECT (MPS) imaging improves visual inter-observer correlation and agreement. Journal of Nuclear Cardiology, 2014, 21, 703-711.	2.1	19
252	Comparative Definitions for Moderate-Severe Ischemia in Stress Nuclear, Echocardiography, and Magnetic Resonance Imaging. JACC: Cardiovascular Imaging, 2014, 7, 593-604.	5.3	168

#	Article	IF	CITATIONS
253	New Hardware Solutions for Cardiac SPECT Imaging. Current Cardiovascular Imaging Reports, 2013, 6, 305-313.	0.6	1
254	State of the Art Hybrid Technology: PET/CT. Current Cardiovascular Imaging Reports, 2013, 6, 328-337.	0.6	1
255	High-efficiency SPECT MPI: Comparison of automated quantification, visual interpretation, and coronary angiography. Journal of Nuclear Cardiology, 2013, 20, 763-773.	2.1	53
256	Improved accuracy of myocardial perfusion SPECT for detection of coronary artery disease by machine learning in a large population. Journal of Nuclear Cardiology, 2013, 20, 553-562.	2.1	122
257	Gated SPECT in assessment of regional and global left ventricular function: An update. Journal of Nuclear Cardiology, 2013, 20, 1118-1143.	2.1	30
258	The amount of dysfunctional but viable myocardium predicts long-term survival in patients with ischemic cardiomyopathy and left ventricular dysfunction. International Journal of Cardiovascular Imaging, 2013, 29, 1645-1653.	1.5	32
259	Relationship of epicardial fat volume to coronary plaque, severe coronary stenosis, and high-risk coronary plaque features assessed by coronary CT angiography. Journal of Cardiovascular Computed Tomography, 2013, 7, 125-132.	1.3	56
260	Quantification of Myocardial Perfusion Reserve Using Dynamic SPECT Imaging in Humans: A Feasibility Study. Journal of Nuclear Medicine, 2013, 54, 873-879.	5.0	200
261	Automated knowledgeâ€based detection of nonobstructive and obstructive arterial lesions from coronary CT angiography. Medical Physics, 2013, 40, 041912.	3.0	19
262	Myocardial perfusion imaging with PET. Imaging in Medicine, 2013, 5, 35-46.	0.0	52
263	Comparison of Fully Automated Computer Analysis and Visual Scoring for Detection of Coronary Artery Disease from Myocardial Perfusion SPECT in a Large Population. Journal of Nuclear Medicine, 2013, 54, 221-228.	5.0	96
264	Multisoftware Reproducibility Study of Stress and Rest Myocardial Blood Flow Assessed with 3D Dynamic PET/CT and a 1-Tissue-Compartment Model of <sup>82</sup> Rb Kinetics. Journal of Nuclear Medicine, 2013, 54, 571-577.	5.0	110
265	Improved Accuracy of Myocardial Perfusion SPECT for the Detection of Coronary Artery Disease Using a Support Vector Machine Algorithm. Journal of Nuclear Medicine, 2013, 54, 549-555.	5.0	69
266	Myocardial Perfusion Imaging with a Solid-State Camera: Simulation of a Very Low Dose Imaging Protocol. Journal of Nuclear Medicine, 2013, 54, 373-379.	5.0	100
267	Combining active appearance and deformable superquadric models for LV segmentation in cardiac MRI. , 2013, , .		4
268	Direct Quantification of Left Ventricular Motion and Thickening Changes Using Rest–Stress Myocardial Perfusion SPECT. Journal of Nuclear Medicine, 2012, 53, 1392-1400.	5.0	18
269	Comparison of Clinical Tools for Measurements of Regional Stress and Rest Myocardial Blood Flow Assessed with <sup>13</sup> N-Ammonia PET/CT. Journal of Nuclear Medicine, 2012, 53, 171-181.	5.0	105
270	Coronary Arterial <sup>18</sup> F-FDG Uptake by Fusion of PET and Coronary CT Angiography at Sites of Percutaneous Stenting for Acute Myocardial Infarction and Stable Coronary Artery Disease. Journal of Nuclear Medicine, 2012, 53, 575-583.	5.0	96

#	Article	IF	CITATIONS
271	Automated detection of contractile abnormalities from stress-rest motion changes. , 2012, 2012, .		0
272	Epicardial fat volume and concurrent presence of both myocardial ischemia and obstructive coronary artery disease. Atherosclerosis, 2012, 221, 422-426.	0.8	67
273	Baseline stress myocardial perfusion imaging results and outcomes in patients with stable ischemic heart disease randomized to optimal medical therapy with or without percutaneous coronary intervention. American Heart Journal, 2012, 164, 243-250.	2.7	175
274	Prognostic value of quantitative high-speed myocardial perfusion imaging. Journal of Nuclear Cardiology, 2012, 19, 1113-1123.	2.1	39
275	Low-dose 3D 82Rb PET. Journal of Nuclear Cardiology, 2012, 19, 1110-1112.	2.1	2
276	CT Quantification of Epicardial Fat: Implications for Cardiovascular Risk Assessment. Current Cardiovascular Imaging Reports, 2012, 5, 352-359.	0.6	6
277	Left ventricular dyssynchrony assessed by gated SPECT phase analysis is an independent predictor of death in patients with advanced coronary artery disease and reduced left ventricular function not undergoing cardiac resynchronization therapy. European Journal of Nuclear Medicine and Molecular Imaging. 2012. 39. 1561-1569.	6.4	42
278	Advances in Nuclear Cardiac Instrumentation with a View Towards Reduced Radiation Exposure. Current Cardiology Reports, 2012, 14, 208-216.	2.9	63
279	Automated quantitative Rb-82 3D PET/CT myocardial perfusion imaging: Normal limits and correlation with invasive coronary angiography. Journal of Nuclear Cardiology, 2012, 19, 265-276.	2.1	55
280	Fully automated wall motion and thickening scoring system for myocardial perfusion SPECT: Method development and validation in large population. Journal of Nuclear Cardiology, 2012, 19, 291-302.	2.1	29
281	Quantitative analysis of perfusion studies: Strengths and pitfalls. Journal of Nuclear Cardiology, 2012, 19, 338-346.	2.1	48
282	Tracking a therapeutic response: How reliable are serial measurements of LV perfusion and function?. Journal of Nuclear Cardiology, 2012, 19, 360-363.	2.1	13
283	Transient ischemic dilation for coronary artery disease in quantitative analysis of same-day sestamibi myocardial perfusion SPECT. Journal of Nuclear Cardiology, 2012, 19, 465-473.	2.1	49
284	Automatic alignment of myocardial perfusion PET and 64-slice coronary CT angiography on hybrid PET/CT. Journal of Nuclear Cardiology, 2012, 19, 482-491.	2.1	21
285	Improvement in PET myocardial perfusion image quality and quantification with flurpiridaz F 18. Journal of Nuclear Cardiology, 2012, 19, 38-45.	2.1	34
286	Reproducibility of myocardial perfusion reserve - variations in measurements from post processing using commercially available software. Cardiovascular Diagnosis and Therapy, 2012, 2, 268-77.	1.7	19
287	Interscan reproducibility of computer-aided epicardial and thoracic fat measurement from noncontrast cardiac CT. Journal of Cardiovascular Computed Tomography, 2011, 5, 172-179.	1.3	51
288	Vulnerable plaque features on coronary CT angiography as markers of inducible regional myocardial hypoperfusion from severe coronary artery stenoses. Atherosclerosis, 2011, 219, 588-595.	0.8	79

#	Article	IF	CITATIONS
289	Automatic 3D registration of dynamic stress and rest <sup>82</sup> Rb and flurpiridaz F 18 myocardial perfusion PET data for patient motion detection and correction. Medical Physics, 2011, 38, 6313-6326.	3.0	34
290	Motion frozen 18F-FDG cardiac PET. Journal of Nuclear Cardiology, 2011, 18, 259-266.	2.1	40
291	Prognostic value of automated vs visual analysis for adenosine stress myocardial perfusion SPECT in patients without prior coronary artery disease: A case-control study. Journal of Nuclear Cardiology, 2011, 18, 1003-1009.	2.1	20
292	Nonlinear registration of serial coronary CT angiography (CCTA) for assessment of changes in atherosclerotic plaque. Medical Physics, 2010, 37, 885-896.	3.0	2
293	Impact of carbohydrate restriction with and without fatty acid loading on myocardial 18F-FDG uptake during PET: A randomized controlled trial. Journal of Nuclear Cardiology, 2010, 17, 286-291.	2.1	104
294	Supine acceptance of a conventional imaging position may make you less prone to success. Journal of Nuclear Cardiology, 2010, 17, 16-18.	2.1	7
295	Enhanced definition PET for cardiac imaging. Journal of Nuclear Cardiology, 2010, 17, 414-426.	2.1	41
296	Combined quantitative analysis of attenuation corrected and non-corrected myocadial perfusion SPECT: Method development and clinical validation. Journal of Nuclear Cardiology, 2010, 17, 591-599.	2.1	49
297	Assessment of the relationship between stenosis severity and distribution of coronary artery stenoses on multislice computed tomographic angiography and myocardial ischemia detected by single photon emission computed tomography. Journal of Nuclear Cardiology, 2010, 17, 791-802.	2.1	40
298	Solid-State SPECT technology: fast and furious. Journal of Nuclear Cardiology, 2010, 17, 890-896.	2.1	42
299	Automatic and visual reproducibility of perfusion and function measures for myocardial perfusion SPECT. Journal of Nuclear Cardiology, 2010, 17, 1050-1057.	2.1	77
300	New Imaging Protocols for New Single Photon Emission CT Technologies. Current Cardiovascular Imaging Reports, 2010, 3, 162-170.	0.6	12
301	Functional Impact of Coronary Stenosis Observed on Coronary Computed Tomography Angiography: Comparison with 13N-Ammonia PET. Archives of Medical Research, 2010, 41, 642-648.	3.3	8
302	Quantification of 3D regional myocardial wall thickening from gated magnetic resonance images. Journal of Magnetic Resonance Imaging, 2010, 31, 317-327.	3.4	16
303	Automated algorithm for atlas-based segmentation of the heart and pericardium from non-contrast CT. , 2010, 7623, 762337.		15
304	Quantitative Upright–Supine High-Speed SPECT Myocardial Perfusion Imaging for Detection of Coronary Artery Disease: Correlation with Invasive Coronary Angiography. Journal of Nuclear Medicine, 2010, 51, 1724-1731.	5.0	126
305	Automated Three-dimensional Quantification of Noncalcified Coronary Plaque from Coronary CT Angiography: Comparison with Intravascular US. Radiology, 2010, 257, 516-522.	7.3	177
306	Multicenter Trial of High-Speed Versus Conventional Single-Photon Emission Computed Tomography Imaging. Journal of the American College of Cardiology, 2010, 55, 1965-1974.	2.8	136

#	Article	IF	CITATIONS
307	Pericardial Fat Burden on ECG-Gated Noncontrast CT in Asymptomatic Patients Who Subsequently Experience Adverse Cardiovascular Events. JACC: Cardiovascular Imaging, 2010, 3, 352-360.	5.3	210
308	Comparison of the Extent and Severity of Myocardial Perfusion Defects Measured by CT Coronary Angiography and SPECT Myocardial Perfusion Imaging. JACC: Cardiovascular Imaging, 2010, 3, 1010-1019.	5.3	68
309	Increased Pericardial Fat Volume Measured From Noncontrast CT Predicts Myocardial Ischemia by SPECT. JACC: Cardiovascular Imaging, 2010, 3, 1104-1112.	5.3	133
310	Computer-aided non-contrast CT-based quantification of pericardial and thoracic fat and their associations with coronary calcium and metabolic syndrome. Atherosclerosis, 2010, 209, 136-141.	0.8	123
311	Improved Quantification and Normal Limits for Myocardial Perfusion Stress–Rest Change. Journal of Nuclear Medicine, 2010, 51, 204-209.	5.0	14
312	Digital/Fast SPECT. , 2010, , 132-148.		3
313	Comparative Use of Radionuclide Stress Testing, Coronary Artery Calcium Scanning, and Noninvasive Coronary Angiography for Diagnostic and Prognostic Cardiac Assessment. , 2010, , 233-254.		Ο
314	Geometric featureâ€based multimodal image registration of contrastâ€enhanced cardiac CT with gated myocardial perfusion SPECT. Medical Physics, 2009, 36, 5467-5479.	3.0	21
315	Automated multi-modality registration of 64-slice coronary CT angiography with myocardial perfusion spect. , 2009, , 358-361.		2
316	Feature-based non-rigid volume registration of serial coronary CT angiography. , 2009, , .		0
317	Automated Quality Control for Segmentation of Myocardial Perfusion SPECT. Journal of Nuclear Medicine, 2009, 50, 1418-1426.	5.0	48
318	Are Shades of Gray Prognostically Useful in Reporting Myocardial Perfusion Single-Photon Emission Computed Tomography?. Circulation: Cardiovascular Imaging, 2009, 2, 290-298.	2.6	46
319	Quantitative Analysis of Myocardial Perfusion SPECT Anatomically Guided by Coregistered 64-Slice Coronary CT Angiography. Journal of Nuclear Medicine, 2009, 50, 1621-1630.	5.0	76
320	Non-Rigid Ultrasound Image Registration Based on Intensity and Local Phase Information. Journal of Signal Processing Systems, 2009, 54, 33-43.	2.1	26
321	Quantitative assessment of myocardial perfusion abnormality on SPECT myocardial perfusion imaging is more reproducible than expert visual analysis. Journal of Nuclear Cardiology, 2009, 16, 45-53.	2.1	139
322	The importance of population-specific normal database for quantification of myocardial ischemia: comparison between Japanese 360 and 180-degree databases and a US database. Journal of Nuclear Cardiology, 2009, 16, 422-430.	2.1	57
323	Advances in technical aspects of myocardial perfusion SPECT imaging. Journal of Nuclear Cardiology, 2009, 16, 255-276.	2.1	223
324	Multimodality image registration with software: state-of-the-art. European Journal of Nuclear Medicine and Molecular Imaging, 2009, 36, 44-55.	6.4	91

#	Article	IF	CITATIONS
325	Stress Thallium-201/Rest Technetium-99m Sequential Dual Isotope High-Speed Myocardial Perfusion Imaging. JACC: Cardiovascular Imaging, 2009, 2, 273-282.	5.3	138
326	Automated 3-dimensional quantification of noncalcified and calcified coronary plaque from coronary CT angiography. Journal of Cardiovascular Computed Tomography, 2009, 3, 372-382.	1.3	100
327	Comparative roles of cardiac CT and nuclear cardiology in assessment of the patient with suspected coronary artery disease. Journal of Invasive Cardiology, 2009, 21, 352-8.	0.4	4
328	Quantitative myocardial-perfusion SPECT: Comparison of three state-of-the-art software packages. Journal of Nuclear Cardiology, 2008, 15, 27-34.	2.1	55
329	Letter to the editor. Journal of Nuclear Cardiology, 2008, 15, 476.	2.1	3
330	Predicting success of prospective and retrospective gating with dual-source coronary computed tomography angiography: Development of selection criteria and initial experience. Journal of Cardiovascular Computed Tomography, 2008, 2, 81-90.	1.3	51
331	Image quality and artifacts in coronary CT angiography with dual-source CT: Initial clinical experience. Journal of Cardiovascular Computed Tomography, 2008, 2, 105-114.	1.3	42
332	Algorithm for radiation dose reduction with helical dual source coronary computed tomography angiography in clinical practice. Journal of Cardiovascular Computed Tomography, 2008, 2, 311-322.	1.3	57
333	Quantitative Diagnostic Performance of Myocardial Perfusion SPECT with Attenuation Correction in Women. Journal of Nuclear Medicine, 2008, 49, 915-922.	5.0	37
334	Optimal Medical Therapy With or Without Percutaneous Coronary Intervention to Reduce Ischemic Burden. Circulation, 2008, 117, 1283-1291.	1.6	1,478
335	Motion-Frozen Myocardial Perfusion SPECT Improves Detection of Coronary Artery Disease in Obese Patients. Journal of Nuclear Medicine, 2008, 49, 1075-1079.	5.0	35
336	Response to Letters Regarding Article, "Optimal Medical Therapy With or Without Percutaneous Coronary Intervention to Reduce Ischemic Burden: Results From the Clinical Outcomes Utilizing Revascularization and Aggressive Drug Evaluation (COURAGE) Trial Nuclear Substudy― Circulation, 2008, 118, .	1.6	1
337	Comparison of Myocardial Perfusion <sup>82</sup> Rb PET Performed with CT- and Transmission CT–Based Attenuation Correction. Journal of Nuclear Medicine, 2008, 49, 1992-1998.	5.0	39
338	Applications and software techniques for integrated cardiac multimodality imaging. Expert Review of Cardiovascular Therapy, 2008, 6, 27-41.	1.5	16
339	High definition PET for cardiac imaging: Preliminary results. , 2008, , .		0
340	Automated Quantitation of Pericardiac Fat From Noncontrast CT. Investigative Radiology, 2008, 43, 145-153.	6.2	90
341	Patient motion correction for multiplanar, multi-breath-hold cardiac cine MR imaging. Journal of Magnetic Resonance Imaging, 2007, 25, 965-973.	3.4	22
342	Quantitation of infarct size in patients with chronic coronary artery disease using rest-redistribution Tl-201 myocardial perfusion SPECT: Correlation with contrast-enhanced cardiac magnetic resonance. Journal of Nuclear Cardiology, 2007, 14, 59-67.	2.1	8

#	Article	IF	CITATIONS
343	Attenuation correction in cardiac SPECT: The boy who cried wolf?. Journal of Nuclear Cardiology, 2007, 14, 25-35.	2.1	39
344	Underestimation of extent of ischemia by gated SPECT myocardial perfusion imaging in patients with left main coronary artery disease. Journal of Nuclear Cardiology, 2007, 14, 521-528.	2.1	310
345	Recent technologic advances in nuclear cardiology. Journal of Nuclear Cardiology, 2007, 14, 501-513.	2.1	109
346	Quantitation in gated perfusion SPECT imaging: The Cedars-Sinai approach. Journal of Nuclear Cardiology, 2007, 14, 433-454.	2.1	219
347	Combined quantitative supine-prone myocardial perfusion SPECT improves detection of coronary artery disease and normalcy rates in women. Journal of Nuclear Cardiology, 2007, 14, 44-52.	2.1	50
348	Left ventricular shape index assessed by gated stress myocardial perfusion SPECT: Initial description of a new variable. Journal of Nuclear Cardiology, 2006, 13, 652-659.	2.1	38
349	Simplified normal limits and automated quantitative assessment for attenuation-corrected myocardial perfusion SPECT. Journal of Nuclear Cardiology, 2006, 13, 642-651.	2.1	51
350	Gated myocardial perfusion single photon emission computed tomography in the clinical outcomes utilizing revascularization and aggressive drug evaluation (COURAGE) trial, Veterans Administration Cooperative study no. 424. Journal of Nuclear Cardiology, 2006, 13, 685-698.	2.1	34
351	Diagnostic accuracy of gated Tc-99m sestamibi stress myocardial perfusion SPECT with combined supine and prone acquisitions to detect coronary artery disease in obese and nonobese patients. Journal of Nuclear Cardiology, 2006, 13, 191-201.	2.1	72
352	Direct quantitative in vivo comparison of calcified atherosclerotic plaque on vascular MRI and CT by multimodality image registration. Journal of Magnetic Resonance Imaging, 2006, 23, 345-354.	3.4	16
353	Rapid Assessment of Left Ventricular Segmental Wall Motion, Ejection Fraction, and Volumes with Single Breath-Hold, Multi-Slice TrueFISP MR Imaging. Journal of Cardiovascular Magnetic Resonance, 2006, 8, 435-444.	3.3	8
354	Combined supine and prone quantitative myocardial perfusion SPECT: method development and clinical validation in patients with no known coronary artery disease. Journal of Nuclear Medicine, 2006, 47, 51-8.	5.0	89
355	Roles of nuclear cardiology, cardiac computed tomography, and cardiac magnetic resonance: assessment of patients with suspected coronary artery disease. Journal of Nuclear Medicine, 2006, 47, 74-82.	5.0	85
356	Automated quantification of myocardial perfusion SPECT using simplified normal limits. Journal of Nuclear Cardiology, 2005, 12, 66-77.	2.1	252
357	Techniques for efficient, real-time, 3D visualization of multi-modality cardiac data using consumer graphics hardware. Computerized Medical Imaging and Graphics, 2005, 29, 463-475.	5.8	25
358	Automatic detection and size quantification of infarcts by myocardial perfusion SPECT: clinical validation by delayed-enhancement MRI. Journal of Nuclear Medicine, 2005, 46, 728-35.	5.0	23
359	Automated image registration of gated cardiac single-photon emission computed tomography and magnetic resonance imaging. Journal of Magnetic Resonance Imaging, 2004, 19, 283-290.	3.4	34
360	Acceleration of 3D, nonlinear warping using standard video graphics hardware: implementation and initial validation. Computerized Medical Imaging and Graphics, 2004, 28, 471-483.	5.8	14

#	Article	IF	CITATIONS
361	Software approach to merging molecular with anatomic information. Journal of Nuclear Medicine, 2004, 45 Suppl 1, 36S-45S.	5.0	25
362	Automatic quantification of myocardial perfusion stress-rest change: a new measure of ischemia. Journal of Nuclear Medicine, 2004, 45, 183-91.	5.0	60
363	"Motion-frozen" display and quantification of myocardial perfusion. Journal of Nuclear Medicine, 2004, 45, 1128-34.	5.0	72
364	Quantification of serial changes in myocardial perfusion. Journal of Nuclear Medicine, 2004, 45, 1978-80.	5.0	11
365	Interactive volume rendering of multimodality 4D cardiac data with the use of consumer graphics hardware. , 2003, 5029, 119.		6
366	Automated 3-dimensional registration of stand-alone (18)F-FDG whole-body PET with CT. Journal of Nuclear Medicine, 2003, 44, 1156-67.	5.0	61
367	Reversible ischemia around intracerebral hemorrhage: a single-photon emission computerized tomography study. Journal of Neurosurgery, 2002, 96, 736-741.	1.6	89
368	Cannabis induced dopamine release: an in-vivo SPECT study. Psychiatry Research - Neuroimaging, 2001, 107, 173-177.	1.8	156
369	Evaluation of voxel-based registration of 3-D power Doppler ultrasound and 3-D magnetic resonance angiographic images of carotid arteries. Ultrasound in Medicine and Biology, 2001, 27, 945-955.	1.5	67
370	Subjective Effects of AMPT-induced Dopamine Depletion in Schizophrenia Correlation between Dysphoric Responses and Striatal D2 Binding Ratios on SPECT Imaging. Neuropsychopharmacology, 2001, 25, 642-650.	5.4	80
371	Evaluation of linear registration algorithms for brain SPECT and the errors due to hypoperfusion lesions. Medical Physics, 2001, 28, 1660-1668.	3.0	62
372	Anatomical validation of automatic respiratory motion correction for coronary 18Fâ€sodium fluoride positron emission tomography by expert measurements from fourâ€dimensional computed tomography. Medical Physics, 0, , .	3.0	4